
FastFLUX: Pruning FLUX with Block-wise Replacement and Sandwich Training

Fuhan Cai^{1,*} Yong Guo^{2,*} Jie Li^{2,*} Wenbo Li³ Xiangzhong Fang¹ Jian Chen²

¹Shanghai Jiao Tong University

²South China University of Technology

³Chinese University of Hong Kong

Abstract

Recent advancements in text-to-image (T2I) generation have led to the emergence of highly expressive models such as diffusion transformers (DiTs), exemplified by FLUX. However, their massive parameter sizes lead to slow inference, high memory usage, and poor deployability. Existing acceleration methods (e.g., single-step distillation and attention pruning) often suffer from significant performance degradation and incur substantial training costs. To address these limitations, we propose **FastFLUX**, an architecture-level pruning framework designed to enhance the inference efficiency of FLUX. At its core is the **Block-wise Replacement with Linear Layers (BRLL)** method, which replaces structurally complex residual branches in ResBlocks with lightweight linear layers while preserving the original shortcut connections for stability. Furthermore, we introduce **Sandwich Training (ST)**, a localized fine-tuning strategy that leverages LoRA to supervise neighboring blocks, mitigating performance drops caused by structural replacement. Experiments show that our FastFLUX maintains high image quality under both qualitative and quantitative evaluations, while significantly improving inference speed, even with 20% of the hierarchy pruned. Our code will be available soon.

1 Introduction

Recent advances in diffusion-based generative models[1, 2, 3, 4, 5, 6, 7, 8] have led to unprecedented progress in high-fidelity image synthesis. Among these, transformer-based architectures such as DiT [9] and FLUX [10] have demonstrated strong generative capabilities by stacking deep and complex hierarchical blocks. These models often rely on extensive depth and repeated structural modules to enhance expressiveness and scalability. However, such architectural designs come at a cost: high computational complexity, large memory footprints, and latency issues that hinder real-time applications and deployment on resource-constrained platforms.

Although prior studies[11, 12, 13, 14, 15, 16, 17, 18, 19, 20] have investigated model compression through pruning, knowledge distillation, and lightweight network design, these approaches typically regard the model as a black box or focus solely on parameter-level sparsity. Few methods[21] explicitly target hierarchical redundancy, an underexplored and distinct source of inefficiency in deep generative transformers. In addition, many existing techniques[22, 23, 24, 25, 26, 27, 28, 29, 30] require training from scratch or result in significant performance degradation, which restricts their applicability in practical deployment scenarios.

In this work, we revisit the challenge of structural redundancy in deep generative models and propose **FastFLUX**, a general and efficient framework for architecture-level compression. It operates by selectively replacing redundant and computationally heavy residual blocks with lightweight linear al-

*Equal Contribution.

ternatives, while maintaining generation quality through an efficient fine-tuning strategy. Specifically, we introduce the **Block-wise Replacement with Linear Layers (BRL)** method, which targets the high-parameter residual branches in ResBlocks. In FLUX, each ResBlock consists of a heavy residual branch and a lightweight shortcut branch. We observe that the residual branches dominate computational cost and significantly slow down inference. BRL replaces these branches with simple linear layers while preserving the original shortcut connections to retain critical information flow and ensure model stability. These replacements can be initialized via least squares estimation, allowing for training-free deployment with controllable performance degradation. To further reduce performance drop after replacement, we propose a **Sandwich Training (ST)** strategy. Rather than fine-tuning the entire model, ST performs localized adaptation for each replaced block by leveraging information from adjacent unpruned layers. During the training of a specific replaced block, we apply LoRA[31] modules to its neighboring layers, forming a “sandwich” structure around the linear module. This localized supervision enables the linear layer to adapt more effectively within its context, leading to better stability and quality with minimal training overhead. Using this approach, we can prune 20% of the FLUX model while maintaining high-quality image generation. The resulting model achieves significantly faster inference with only minimal performance degradation.

To sum up, the **contributions** of this paper are:

- We propose **FastFLUX**, a novel architecture-level pruning framework built upon the 12B FLUX model. FastFLUX is lightweight, efficient, and incurs low training cost. Even under a 20% pruning ratio, it maintains high visual generation quality.
- We introduce **Block-wise Replacement with Linear Layers (BRL)**, which replaces complex residual branches with linear layers. These replacements support least squares initialization, enabling training-free deployment with controlled performance loss.
- We propose **Sandwich Training (ST)** strategy to compensate for performance loss after pruning. This method performs localized fine-tuning by applying LoRA modules to the neighboring layers of each replaced block, enabling efficient and targeted adaptation with minimal training overhead.

2 Related Work

Diffusion-based Generative Models. Recent advances in diffusion models have led to impressive progress in image generation and editing. Approaches such as DDPM [32], Latent Diffusion [33], and DiT [9] demonstrate strong scalability by employing deeply stacked hierarchical modules. While these architectures enhance generative capacity, they also introduce substantial computational overhead. More recent models like FLUX [10] further deepen the Transformer backbone to boost fidelity, which underscores the growing need for structural efficiency and optimization in diffusion-based generation systems. This motivates a closer investigation into architectural redundancy and the development of efficient simplification strategies that can accelerate inference while preserving image quality.

Model Compression and Pruning. Mainstream compression techniques include knowledge distillation [34], quantization [35], and neural architecture search [36]. Unstructured pruning removes individual weights based on importance scores but typically results in irregular sparse patterns, which are difficult to accelerate on standard hardware without customized sparse kernels. In contrast, structured pruning [37, 38] simplifies the model by removing entire filters, channels, or blocks, offering better compatibility with existing hardware. However, few existing methods explicitly address the depth-wise redundancy of transformer-based generative models, especially in diffusion architectures, where deeply stacked structures are prevalent but costly.

Efficient Transformer and Block Simplification. Efficient Transformer variants [39, 40] aim to reduce attention complexity through sparse or linear approximations, but primarily focus on token-level interactions rather than architectural depth. Other efforts simplify vision transformers by employing early exiting [41, 42], layer dropping [43], or block merging [44], highlighting the unequal contribution of layers across depth. Recent works on structural adaptation [45, 46] further demonstrate the importance of depth-aware design, revealing that static layer stacks are often suboptimal. Building on these insights, our method evaluates block-level importance via gradient-based and output-sensitivity analysis, enabling selective pruning or replacement of redundant layers in deep diffusion models while preserving generation quality.

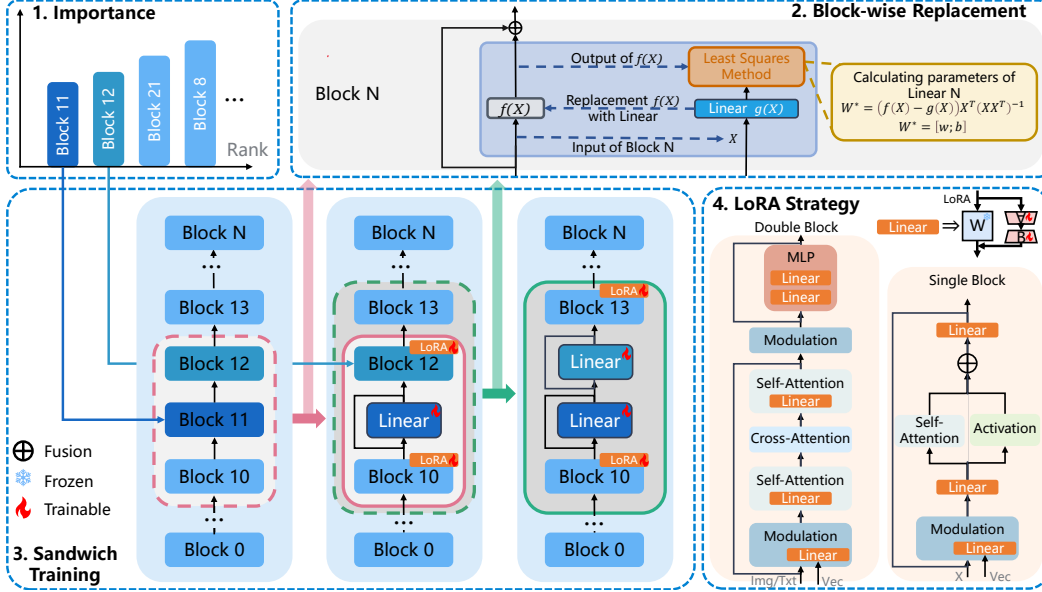


Figure 1: Overview of the FastFLUX Framework. **(1) Importance Estimation:** We compute the importance of each block and prioritize pruning of less important ones. **(2) Block-wise Replacement with Linear Layers (BRLL):** For each selected block, we replace its residual branch with a lightweight linear layer. The parameters of the linear layer are computed using the least squares method based on input-output pairs collected during forward inference. **(3) Sandwich Training (ST):** For non-overlapping cases, we train the replaced block along with its immediate neighbors enhanced by LoRA. For overlapping cases, we search upward or downward to locate the nearest unpruned blocks, apply LoRA to those, and jointly train all intermediate replaced blocks. Input-output data for each training step are re-collected by loading all previously trained sandwich structures. **(4) LoRA Strategy:** LoRA modules are selectively inserted into either single or double blocks during sandwich training to provide local supervision while keeping the rest of the model frozen. This framework enables efficient and structured pruning with minimal performance degradation.

3 FastFLUX: Block-wise Efficient Pruning with Sandwich Training

FastFLUX is designed to prune large-scale diffusion transformers in a lightweight and effective manner, improving inference efficiency while maintaining generation quality. In this section, we provide a complete description of our proposed pruning framework. In Section 3.1, we introduce **Block-wise Replacement with Linear Layers (BRLL)**, which replace the residual branches of ResBlocks with simplified linear modules while preserving shortcut connections to retain key representational capacity. In Section 3.2, we present **Sandwich Training (ST)**, a localized fine-tuning strategy that leverages LoRA-based supervision to compensate for potential performance loss after pruning, while maintaining high training efficiency. The overall workflow and implementation details of FastFLUX are illustrated in Figure 1 and Algorithm 1.

3.1 Block-wise Replacement with Linear Layer

To compress ultra-large models like FLUX and improve their inference efficiency, we propose an architecture-level pruning strategy called BRLL, which targets the internal residual structure of the model. We observe that FLUX consists of a large number of repeated ResBlocks with high parameter counts. Each ResBlock typically contains two branches: a computationally heavy residual branch and a lightweight shortcut branch. Our analysis indicates that the residual branch is the primary contributor to the model’s high computational cost and slow inference speed. Motivated by this, we propose to replace the residual branches with lightweight linear layers, while preserving the original shortcut connections during the replacement process. Although it is possible to replace the entire ResBlock with a single linear layer, we find that doing so leads to noticeable performance degradation, as the shortcut connection carries essential identity information. Therefore, our method selectively

Algorithm 1: Block-wise Replacement with Linear Layer and Sandwich Training.

Require : Pretrained FLUX model, replacement ratio $r \in [0, 1]$, the number of blocks in the model N , the weight of FID in computing the importance score α , the weight of CLIP score in computing the importance score β .

Output : Pruned model with replaced linear blocks

for each block B_i **do**

 Temporarily remove B_i and conduct forward propagation on benchmark datasets;
 Compute FID and CLIP score;
 Compute the importance score $s_i = \alpha\text{FID} + \beta\text{CLIP}$;

Sort the importance scores $\{s_i\}_{i=1}^N$ in the ascending order;

Select the top- r least important blocks $\{B_k\}_{k=1}^{rN}$ according to their importance scores;

for each $B_k \in \{B_k\}_{k=1}^{rN}$ **do**

 // Block-wise Replacement with Linear Layer

 Collect the input and output of the residual branch in B_k ;

 Compute the weight of the linear layer that is used to replace the residual branch:

$$W^* = (f(X) - g(X))X^T(XX^T)^{-1}, W^* = [W; b]$$

 // Sandwich Training

 Take B_k as the center and combine the ones before and after it to construct a **sandwich block**;

 Collect the input and output of the sandwich block for finetuning;

 Replace the residual branch of B_k with the linear layer using the weights W^* ;

 Add LoRA into the first and last blocks inside the sandwich block;

 Finetune the sandwich by minimizing the difference between the original and pruned one.

replaces only the residual branch, allowing the shortcut to preserve critical information flow. This distinguishes our approach from prior pruning methods that often disregard the functional asymmetry within ResBlocks. The method is illustrated in Figure 2.

Specifically, let X denote the input to a ResBlock, $f(X)$ the output of its residual branch, and $Y = f(X) + X$ the original output of the ResBlock. To reduce computation while preserving the residual structure, we replace the residual branch with a lightweight linear layer $g(X) = WX + b$, resulting in the modified output $\hat{Y} = g(X) + X$. To preserve the representational behavior of the original block, we minimize the approximation error between the original residual output and its linear approximation. This leads to the following objective: $\min_{W,b} \|f(X) - g(X)\|^2$. The optimal parameters W^* of the linear layer can be obtained from using the least squares method, based on the collected input-output pairs of each ResBlock during forward inference:

$$W^* = (f(X) - g(X))X^T(XX^T)^{-1}, W^* = [W; b]. \quad (1)$$

This procedure yields an initial estimation of the linear layer’s parameters, which can be further optimized during the subsequent training phase of our ST strategy described in Section 3.2.

3.2 Sandwich Training

To further enhance the generation quality of pruned models and bring them closer to the original model’s performance, we propose the **Sandwich Training (ST)** strategy. We observe that different blocks contribute unequally to the model’s performance, and prioritizing the pruning of less important blocks leads to more stable and effective compression. Therefore, we begin this section by introducing a method for **Calculating Block Importance**. Based on the computed importance scores, block pruning may lead to structural overlap between selected regions. To address this, our ST strategy includes dedicated mechanisms for **Training Sandwich Blocks without Overlap** and **with Overlap**, respectively. Finally, in **Inference Reuse from High-Pruned Models**, we present an empirical finding that transferring trained parameters from high-pruned models to lower-pruned configurations can further improve performance without additional training.

Calculating Block Importance. We observe that different blocks contribute unequally to the model’s generative performance (see Section 4.4 for more results). Based on this observation, we adopt an importance-aware pruning strategy that prioritizes the removal of less critical blocks. To

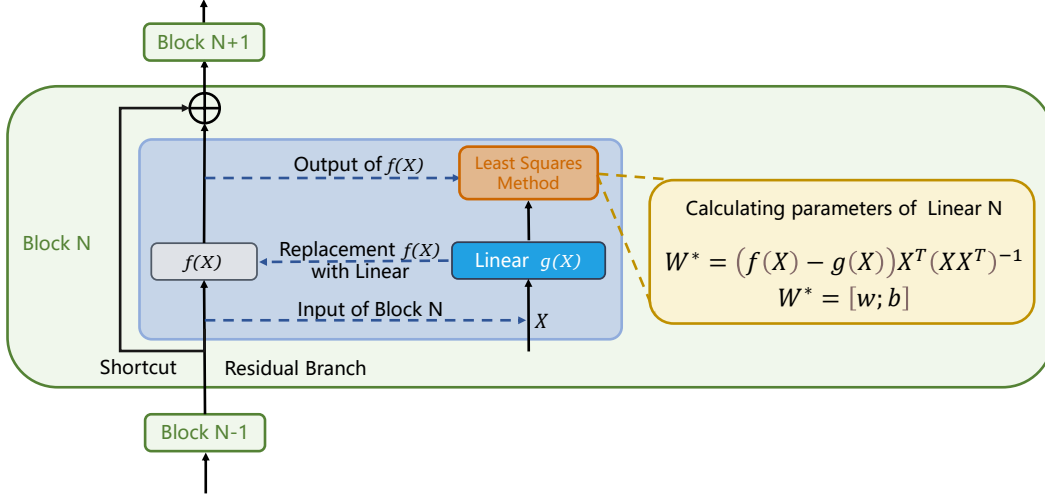


Figure 2: Illustration of the Block-wise Replacement with Linear Layers (BRL) method. Each ResBlock consists of a residual branch and a shortcut branch. The residual branch is replaced with a linear layer, whose parameters are computed using input-output features collected during the forward pass. The shortcut connection is preserved to maintain stable information flow.

quantitatively assess the importance of each block, we combine two commonly used metrics in text-to-image evaluation: FID [47] and CLIP Score [48]. Specifically, for each ResBlock, we temporarily remove it from the model and generate a set of images. We then compute the FID and CLIP scores for each generated set and normalize both scores independently across all blocks. Since a lower FID indicates better quality, we transform it by taking $1 - FID_{norm}$ so that higher values are consistently better across both metrics. The importance score s_i for the i -th block is defined as:

$$s_i = -(\alpha(1 - FID_{norm}^{(i)}) + \beta CLIP_{norm}^{(i)}), \quad (2)$$

where α and β are hyperparameters that balance the contribution of each metric. In our experiments, we set $\alpha = \beta = 0.5$. A lower score s_i implies that removing the block has a smaller impact on the overall generation quality, indicating that the block is less important and should be pruned earlier in the compression process. We sort all the blocks according to their importance scores in ascending order to conduct block replacement.

Training Sandwich Blocks without Overlap. When a ResBlock’s residual branch is replaced with a single linear layer, the number of trainable parameters becomes significantly limited. To better align the pruned model with the original network and mitigate accuracy degradation caused by pruning, we introduce the ST strategy. The key idea is to leverage the neighboring blocks to enhance the training of the locally replaced block. Specifically, when the block to be replaced is \mathbf{B}_i , we first collect training data by recording the input to \mathbf{B}_{i-1} and the output from \mathbf{B}_{i+1} during a forward pass. Then, we isolate three blocks: \mathbf{B}_{i-1} , \mathbf{B}_i , \mathbf{B}_{i+1} . We replace the residual branch of \mathbf{B}_i with a linear layer, apply LoRA to \mathbf{B}_{i-1} and \mathbf{B}_{i+1} , and allow the full parameters of the linear layer in \mathbf{B}_i to be trainable. The structure of the LoRA injection is illustrated in Figure 3. The collected input-output pair forms a localized training dataset. This sandwich-like configuration, where the replaced linear layer is flanked by two LoRA-enhanced blocks, is shown in the Sandwich Training part in Figure 1. Each linear layer is initialized using the solution described in Section 3.1. Before pruning a new block, we reload all previously trained sandwich structures to collect updated input-output pairs from the current model. This ensures that each new sandwich block is trained with data that reflects the latest model state, promoting consistency and stability during progressive pruning. This formulation above applies to the non-overlapping case, where both adjacent blocks have not yet been replaced, i.e., $\mathbf{B}_{i-1} \notin \mathcal{R}$ and $\mathbf{B}_{i+1} \notin \mathcal{R}$, with \mathcal{R} denoting the set of previously replaced blocks. This is shown in the middle column of the Sandwich Training part in Figure 1.

Training Sandwich Blocks with Overlap. When at least one adjacent block of the current block \mathbf{B}_i has already been replaced with a linear layer, that is, $\mathbf{B}_{i-1} \in \mathcal{R}$ or $\mathbf{B}_{i+1} \in \mathcal{R}$, the resulting sandwich structure overlaps with previously replaced blocks. In such cases, we construct an extended sandwich

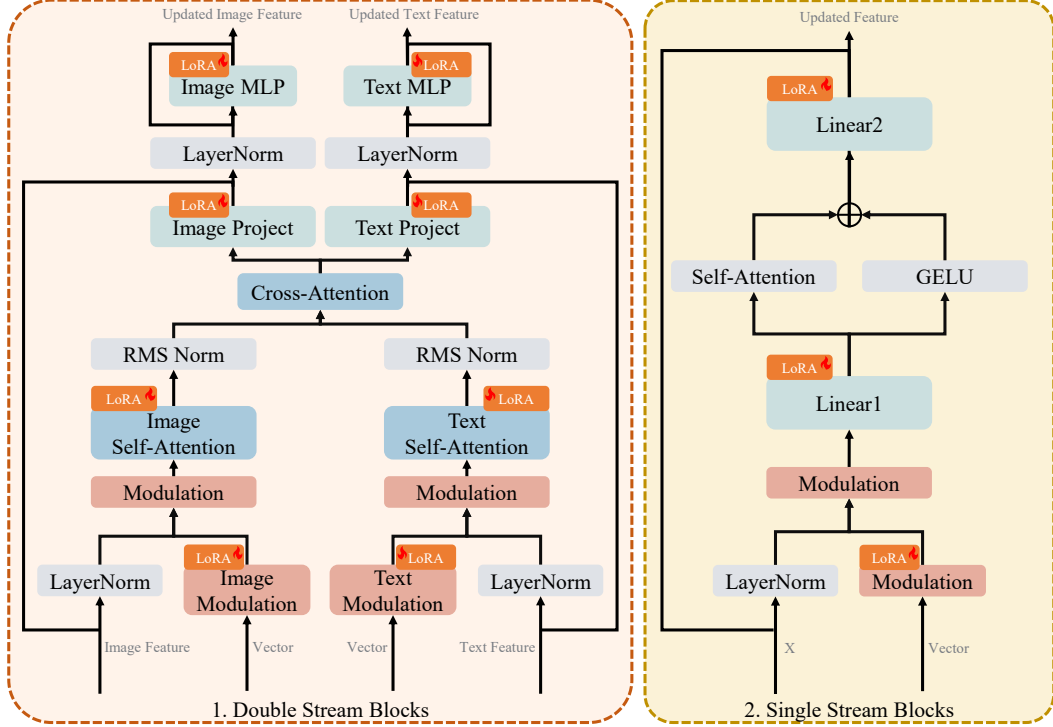


Figure 3: Illustration of the LoRA insertion strategy used in our Sandwich Training (ST). For each block selected for replacement with a linear layer, we identify its closest unpruned neighboring blocks before and after. LoRA modules are inserted into these adjacent blocks to provide localized supervision, enabling efficient and targeted fine-tuning of the replaced block.

structure by identifying the nearest unpruned blocks above and below \mathbf{B}_i and applying LoRA to them. Formally, we define:

$$u = \max \{j < i \mid \mathbf{B}_j \notin \mathcal{R}\}, \quad d = \min \{j > i \mid \mathbf{B}_j \notin \mathcal{R}\} \quad (3)$$

where u and d represent the indices of the nearest unpruned blocks before and after \mathbf{B}_i , respectively. $j \in \mathcal{R}$ refers to a previously replaced block. LoRA modules are applied to \mathbf{B}_u and \mathbf{B}_d , while the linear layer in \mathbf{B}_i , together with all previously replaced linear layers between \mathbf{B}_u and \mathbf{B}_d , are jointly trained using input-output data collected from the model with all prior sandwich structures loaded. The overlap-aware configuration is illustrated in the right column of the ST section in Figure 1.

Inference Reuse from High-Pruned Models. Our training strategy operates in a block-wise manner, where each replacement is optimized locally rather than through end-to-end fine-tuning. This design significantly reduces computational cost and memory consumption. As described earlier, before replacing a new block, we load all previously trained sandwich structures, including both linear layers and LoRA modules, and perform a forward pass to collect the input-output pairs required for training the current block. This ensures that each stage of training is based on the current model state, maintaining pruning stability and minimizing cumulative performance degradation. At inference time, we assemble the final pruned model by incorporating all trained sandwich structures. An interesting phenomenon emerges when components trained under a higher pruning ratio model are reused in a lower pruning ratio configuration. Specifically, after training a model with a pruning ratio of $a\%$, we continue training it to a higher pruning ratio $b\%$, with $b > a$. After the higher pruning stage is completed, we extract the corresponding trained components, including linear layers and LoRA modules, and insert them into the $a\%$ model without any additional fine-tuning. This reuse consistently leads to improved inference performance compared to using only the components trained at the $a\%$ stage. We hypothesize that this improvement arises from block-level overlap across pruning stages. In higher pruning configurations, overlapping blocks participate in multiple sandwich training setups and are therefore updated more frequently with diverse input distributions. This repeated

Table 1: Quantitative comparison on the HPS v2 benchmark. We group models by similar inference latency to fairly compare the effectiveness of FastFLUX and L1-norm pruning at different compression ratios. Results show that FastFLUX achieves better or comparable performance across all categories, and even outperforms the original uncompressed FLUX.1-dev model when pruned by 10 percent. Underlined values indicate the best result in each category across all models, while **bold** values highlight the best result within each latency group.

Model	Animation	Concept-art	Painting	Photo	Averaged	Latency (ms)↓
DALL-E mini[49]	26.10	25.56	25.56	26.12	25.83	-
SD v1.4[50]	27.26	26.61	26.66	27.27	26.95	-
SD v2.0[50]	27.48	26.89	26.86	27.46	27.17	-
SD v3.0[2]	28.58	27.87	28.15	27.72	28.08	-
FLUX.1-dev	28.94	27.90	28.16	28.28	28.32	98.26
FLUX-Pruning-12%	28.83	27.75	28.03	28.21	28.20	89.98
FastFLUX-10%	<u>29.04</u>	<u>28.24</u>	<u>28.49</u>	<u>28.57</u>	<u>28.58</u>	90.78
FLUX-Pruning-21%	28.41	27.39	27.67	27.91	27.84	85.66
FastFLUX-15%	28.58	27.87	28.13	28.19	28.19	85.39
FLUX-Pruning-27%	27.66	26.67	27.03	27.31	27.17	81.98
FastFLUX-20%	28.06	27.48	27.72	27.77	27.76	80.83

Table 2: Quantitative results on the GENEVAL benchmark. We compare two compression methods, FastFLUX and L1-norm pruning, under different pruning ratios. Models with similar inference latency are grouped together for fair comparison. FastFLUX consistently achieves better performance across most categories. Underlined values indicate the best result in each category across all models, while **bold** values highlight the best result within each latency group.

Model	Single object	Two object	Counting	Colors	Position	Attribute binding	Overall	Latency (ms)↓
DALL-E mini[49]	0.73	0.11	0.12	0.37	0.02	0.01	0.23	-
SD v1.4[50]	0.98	0.36	0.35	0.73	0.01	0.07	0.42	-
SD v2.0[50]	0.98	0.50	0.48	0.86	0.06	0.15	0.51	-
SD v3.0[2]	0.98	0.75	0.51	0.84	<u>0.22</u>	<u>0.52</u>	0.63	-
FLUX.1-dev	<u>0.99</u>	<u>0.78</u>	<u>0.70</u>	0.78	0.19	0.46	<u>0.64</u>	98.28
FLUX-Pruning-12%	0.98	0.72	0.59	0.76	0.15	0.40	0.60	90.00
FastFLUX-10%	0.99	0.69	0.63	0.74	0.15	0.42	0.60	90.85
FLUX-Pruning-21%	0.98	0.61	0.54	0.76	0.13	0.29	0.55	85.22
FastFLUX-15%	0.98	0.65	0.56	0.73	0.13	0.35	0.57	85.67
FLUX-Pruning-27%	0.97	0.43	0.44	0.71	0.09	0.19	0.47	81.59
FastFLUX-20%	0.98	0.59	0.48	0.68	0.12	0.31	0.53	80.78

exposure enhances their generalization ability and alignment with the global structure of the model. When reused in the lower pruning configuration, these components offer improved representational capacity and lead to better generation quality without additional training.

4 Experiments

In this section, we experimentally validate the effectiveness and rationality of our proposed method. We begin by introducing the experimental setup and implementation details. Then, we conduct quantitative, qualitative, and efficiency comparisons with existing T2I methods to assess overall performance. Furthermore, we present generalization experiments and ablation studies to provide deeper insights into the design behind FastFLUX. Finally, we include several additional experiments to further strengthen the completeness and logical rigor of our methodology.

4.1 Implementation Details

Our base model is FLUX.1-dev, and all experiments are conducted using the fluxdev-controlnet-16k dataset, which consists of approximately 16.1k images. We sample 512 images to compute the parameters of the linear layers and another 512 images for training. To provide a comprehensive

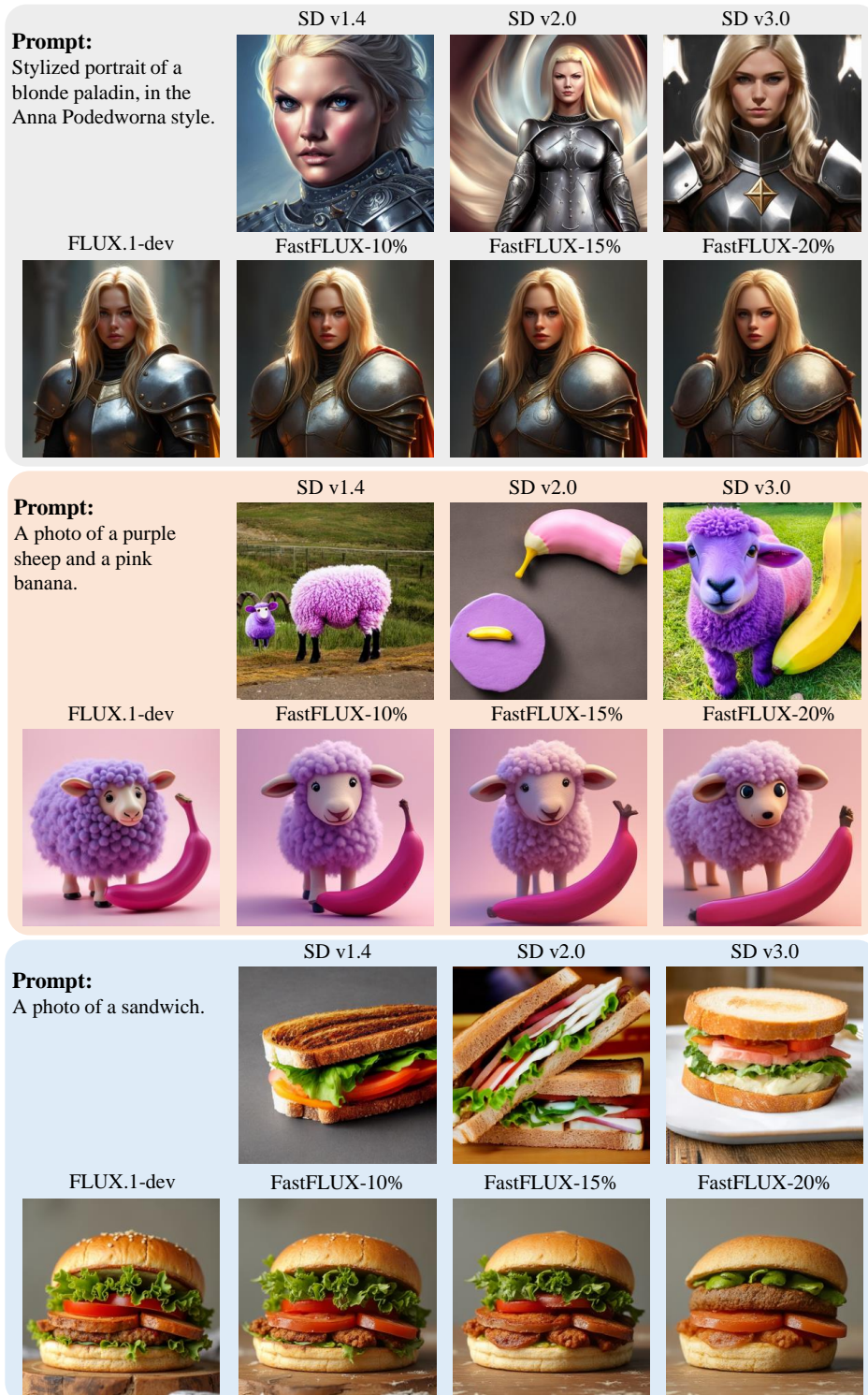
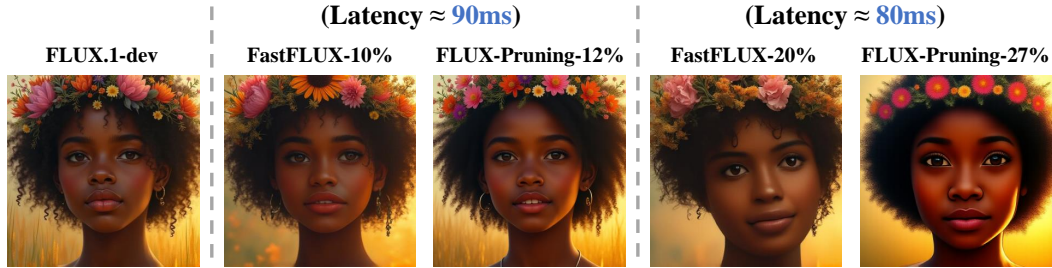


Figure 4: Qualitative comparison between FastFLUX and other mainstream T2I models under the same prompts. FastFLUX consistently generates images of higher visual fidelity. Even at different pruning ratios, the outputs of FastFLUX remain similar to those of the original FLUX.1-dev, while outperforming non-FLUX baselines in overall quality.



Prompt: Oil portrait of a young black woman wearing a wildflower crown in golden light.



Prompt: A photo of a bird.

Figure 5: Qualitative comparison between FastFLUX and L1-norm pruned models under similar latency settings. Within each latency group, FastFLUX achieves better alignment with the original FLUX.1-dev output, preserving more texture and visual detail. In contrast, L1-norm pruned models tend to lose fine-grained information, especially under higher pruning ratios.

and holistic assessment of our method, we utilize a range of text-to-image evaluation benchmarks, including HPS v2 [51] and GENEVAL [52]. All experiments are conducted in PyTorch and run on NVIDIA RTX 3090 GPUs.

4.2 Performance Comparison

Quantitative Results on Multiple Benchmarks. We evaluate the T2I generation performance of our model on two widely used benchmarks: HPS v2 (for assessing alignment with complex human preferences) and GENEVAL (for evaluating short-prompt generation). The results are shown in Table 1 and Table 2, respectively. We compare FastFLUX with the original FLUX.1-dev, L1-norm pruned [53] variants of FLUX, and several state-of-the-art T2I models [50, 2, 49]. Since both FastFLUX and the L1-norm method are model compression techniques, we group models by similar inference latency for fair comparison. From the results, we observe that FastFLUX, when pruned by 10 percent, not only preserves generation quality but also outperforms the original FLUX.1-dev on the HPS v2 benchmark. Specifically, it achieves an improvement of 0.26 in score and ranks first among all evaluated T2I models. In addition, FastFLUX reduces inference latency by 7.48ms compared to the unpruned baseline. Within the same latency group, the L1-norm pruned model removes 12 percent of the parameters but performs 0.38 lower than FastFLUX on the HPS v2 metric. Moreover, L1-based pruning requires global fine-tuning to adapt to the irregular parameter structure, resulting in higher training costs. In contrast, FastFLUX requires only minimal localized adaptation. These observations are consistent across other latency groups and evaluation settings. Overall, FastFLUX significantly improves inference efficiency while maintaining high-quality image generation.

Qualitative Results on Generated Samples. For qualitative evaluation, we present a visual comparison of image generation quality across different models. As shown in Figure 4, FastFLUX consistently produces images of higher quality compared to other mainstream text-to-image models. Among the FastFLUX variants, even under varying pruning ratios, the generated results remain visually similar to those from the original FLUX.1-dev model. Although higher pruning ratios may lead to the loss of fine details, the visual quality of FastFLUX remains superior to that of non-FLUX baselines. In Figure 5, we compare the visual outputs of FastFLUX and the models pruned via L1-norm. When inference latency is almost the same, FastFLUX is able to retain more texture and visual details, showing better alignment with the unpruned model. In contrast, the L1-norm pruned models tend to lose more fine-grained information, especially at higher pruning ratios. These results demonstrate that FastFLUX effectively balances inference efficiency with high-fidelity image generation.

Table 3: Generalization of our method to the SD v3.0 model. The improved CLIP score on FastSD demonstrates that our method remains effective when applied to other text-to-image models beyond the FLUX framework.

Model	HPS v2	CLIP Score
FLUX.1-dev	28.32	31.35
FastFLUX-10%	28.58	30.98
SD v3.0[2]	28.08	31.79
FastSD v3.0-10%	27.76	31.82

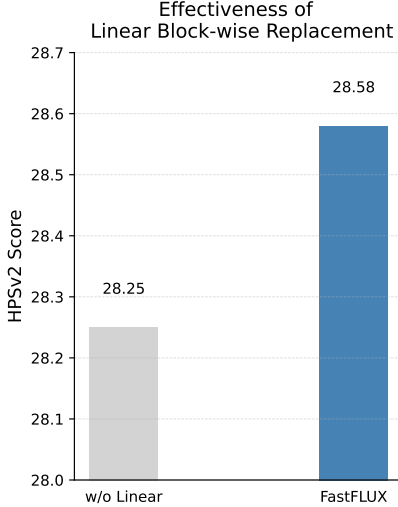


Figure 6: Comparison of HPS v2 scores with and without linear layers, under the same training strategy. The result shows that incorporating BRLl significantly improves performance.

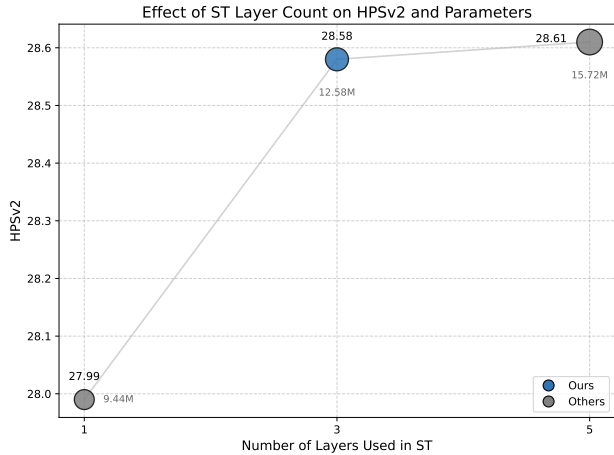


Figure 7: HPS v2 scores under different numbers of layers involved in Sandwich Training. The x-axis indicates the number of layers with LoRA modules applied. The score increases significantly from 1 to 3 layers, then plateaus. A 3-layer structure is adopted as a trade-off between performance and efficiency.

Efficiency Analysis. In Table1 and Table2, we group models with similar inference latency together for fair comparison. The quantitative results show that although latency is comparable, the L1-norm-based pruning approaches are consistently outperformed by our proposed FastFLUX in terms of both image generation quality and pruning effectiveness. Moreover, the L1-norm method requires full model fine-tuning after pruning, which leads to significantly higher training cost. In contrast, FastFLUX achieves a better trade-off between efficiency and quality, making it a more practical and scalable solution for model acceleration.

Generalization to Other Architectures. While FastFLUX is primarily evaluated on the FLUX model with a DiT-style backbone, we further assess its generalization capability on Stable Diffusion v3.0 [2], a model with a different architectural design. Specifically, we apply both BRLl and ST to SD v3.0, which differs in depth, attention layout, and residual structure. As shown in Table 3, the FastSD v3.0-10% variant achieves a higher CLIP Score compared to the unpruned SD v3.0 baseline, with only a moderate drop in HPS v2. These results confirm that BRLl and ST generalize well beyond DiT-style transformers and can benefit other class of diffusion-based generative models.

4.3 Ablation Studies

In this section, we conduct a series of ablation studies to evaluate the key components of our method. These include the impact of block-wise replacement with linear layers, the effect of the proposed sandwich training strategy, the influence of the number of layers used to construct the sandwich block, the impact of different pruning orders, and the performance under varying pruning ratios.

Table 4: Ablation study on the effectiveness of the Sandwich Training (ST) strategy. Without ST, the model applies BRLL to replace residual branches with linear layers using calculated parameters, but without further adaptation. As shown, omitting ST leads to a notable drop in HPS v2 performance.

Method	HPS v2	CLIP Score	Latency (ms)↓
FLUX.1-dev	28.32	31.35	98.26
FastFLUX-10%	28.58	30.98	90.78
w/o ST	27.99	30.91	90.83

Table 5: Comparison of different block replacement orders. Our importance-guided strategy achieves the best performance, while the Strat2End strategy performs worst, likely due to the generally higher importance of double blocks compared to single blocks. See Figure 8 for details.

	FastFLUX	Start2End	End2Strat
HPSv2	28.58	24.63	28.15

Impact of Block-wise Replacement with Linear Layer. To evaluate the necessity of block-wise replacement, we perform a variant where selected low-importance ResBlocks are directly removed without replacement. Specifically, we remove the residual branches of these blocks while preserving the shortcut connections, and apply the same ST strategy as in our full method. As shown in Figure 6, this direct removal leads to a significant drop in performance compared to using linear replacements. The HPSv2 score decreases by 0.33, from 28.58 to 28.25, confirming that the linear replacement step is crucial for preserving model capability after pruning.

Impact of Sandwich Training. We evaluate the effectiveness of the proposed ST strategy by comparing it with a variant that only applies the initialization described in Section 3.1, without any further fine-tuning. As shown in Table 4, removing ST leads to a notable drop in HPS v2 score from 28.58 to 27.99, resulting in a 0.59 degradation. This demonstrates that solely relying on the initial linear approximation is insufficient to fully preserve generative quality. By allowing neighboring blocks with linear replacements to participate in the training process through LoRA modules, the ST strategy introduces localized supervision that helps compensate for performance loss caused by structural pruning. These results confirm that ST is both effective and essential for maintaining model quality under architectural modifications.

Number of layers in Sandwich Block. In FastFLUX, Sandwich Training applies LoRA modules to adjacent blocks around the replaced linear layer to provide localized supervision. We investigate how the number of surrounding layers involved in ST affects model performance. Specifically, using 1 layer means no LoRA is applied. A 3-layer configuration includes LoRA on \mathbf{B}_{i-1} and \mathbf{B}_{i+1} , while a 5-layer setting extends this to \mathbf{B}_{i-2} , \mathbf{B}_{i-1} , \mathbf{B}_{i+1} , and \mathbf{B}_{i+2} . As shown in Figure 7, moving from 1 to 3 layers yields a substantial improvement in HPS v2 score by 0.59, demonstrating the benefit of local supervision from adjacent blocks. However, increasing from 3 to 5 layers results in only a marginal gain 0.03, while introducing a 25% increase in trainable parameters. This diminishing return, coupled with increased computational cost, makes the 3-layer configuration a favorable trade-off between performance and efficiency.

Impact of the Order of Blocks to be Pruned. A key design in FastFLUX is to prioritize pruning blocks with lower estimated importance, thereby minimizing performance degradation. To assess the impact of pruning order, we compare our importance-guided strategy with two sequential baselines: Start2End and End2Start. The former prunes blocks following the data flow direction (from shallow to deep), while the latter does so in the reverse direction. As shown in Table 5, the importance-based strategy achieves the best HPS v2 score of 28.58, outperforming End2Start and Start2End by 0.43 and 3.95 points, respectively. These results demonstrate that the choice of pruning order significantly influences model performance. We hypothesize that pruning in a Start2End fashion may remove low-level blocks that are critical for extracting foundational visual features. In contrast, End2Start pruning disrupts high-level semantics and weakens the gradient signals needed to update shallow layers effectively. FastFLUX avoids these pitfalls by selecting blocks based on calculated importance scores rather than depth. This fine-grained, contribution-aware strategy enables a better balance between compression and generative quality.

Table 6: Performance under different block replacement ratios. As the ratio increased, the reduction in computational complexity and inference time became more significant, while the decrease in HPS v2 was relatively moderate.

Ratio	Drop #Block	FLOPs (T)	Inference Time(ms)	HPSv2
0 (baseline)	0	38.19	98.26	28.32
5%	3	36.79 (96.3%)	93.24	28.23
10%	5	35.87 (93.9%)	90.78	28.58
15%	8	33.39 (87.4%)	85.39	28.19
20%	11	32.46 (85.0%)	80.83	27.76
25%	14	31.07 (81.3%)	76.85	27.10
30%	16	29.37 (76.9%)	72.30	26.70

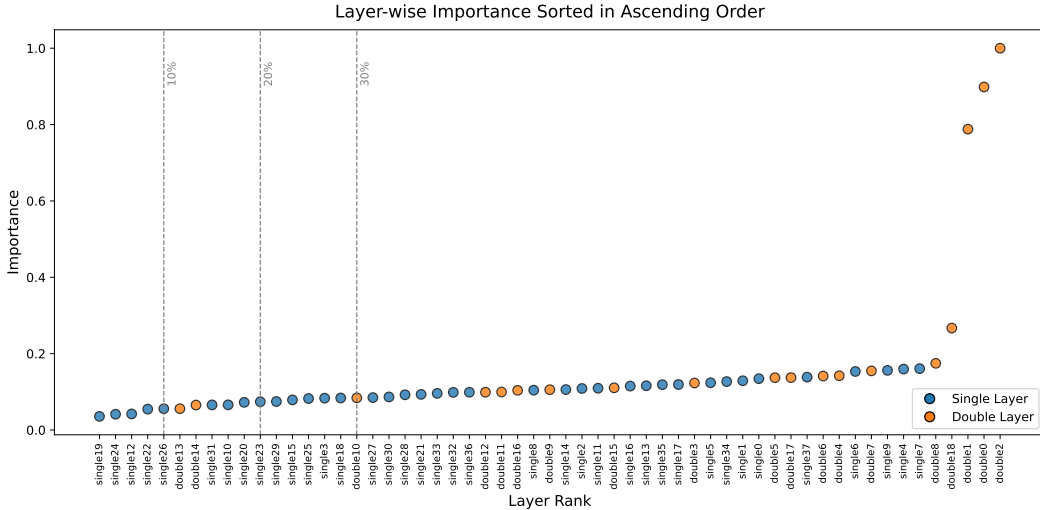


Figure 8: Importance scores of all layers, sorted in ascending order. Each dot represents a layer, with yellow indicating double layers and blue indicating single layers. The dashed vertical lines at 10%, 20%, and 30% mark the thresholds used for Block-wise Replacement with Linear Layers.

Performance with Different Pruning Ratios. We apply FastFLUX to prune the FLUX model under various pruning ratios. As shown in Table 6, increasing the pruning ratio leads to a clear reduction in both computational cost and inference latency. For example, at a 30% pruning ratio, FLOPs are reduced to 76.9% of the original model and inference time drops by 25.96 ms, while the HPS v2 score decreases by only 1.62. A particularly noteworthy observation is the asymmetry between performance degradation and efficiency gain. While inference time and FLOPs decrease significantly with higher pruning ratios, the HPS v2 score remains relatively stable up to a moderate pruning level (e.g., 10–15%). This highlights the efficiency and robustness of the FastFLUX pruning strategy, which enables substantial acceleration with minimal quality loss.

4.4 Additional Experiments

To further support the rationale and effectiveness of our method, we present two complementary experiments. In Layer Importance Analysis, we quantitatively evaluate the contribution of each block to generation quality, providing the basis for our importance-aware pruning strategy. In Visual Analysis of Multiple Replacement Strategies, we qualitatively compare different block replacement methods, demonstrating the visual advantages of combining BRLL with ST.

Layer Importance Analysis. In this part, we provide analysis of layer importance and the impact of different layers to the generation results. The method for computing block importance is detailed in Section 3.2. Figure 8 shows the importance scores of all blocks ranked from low to high. It can be observed that only a few layers have importance scores significantly higher than others. This

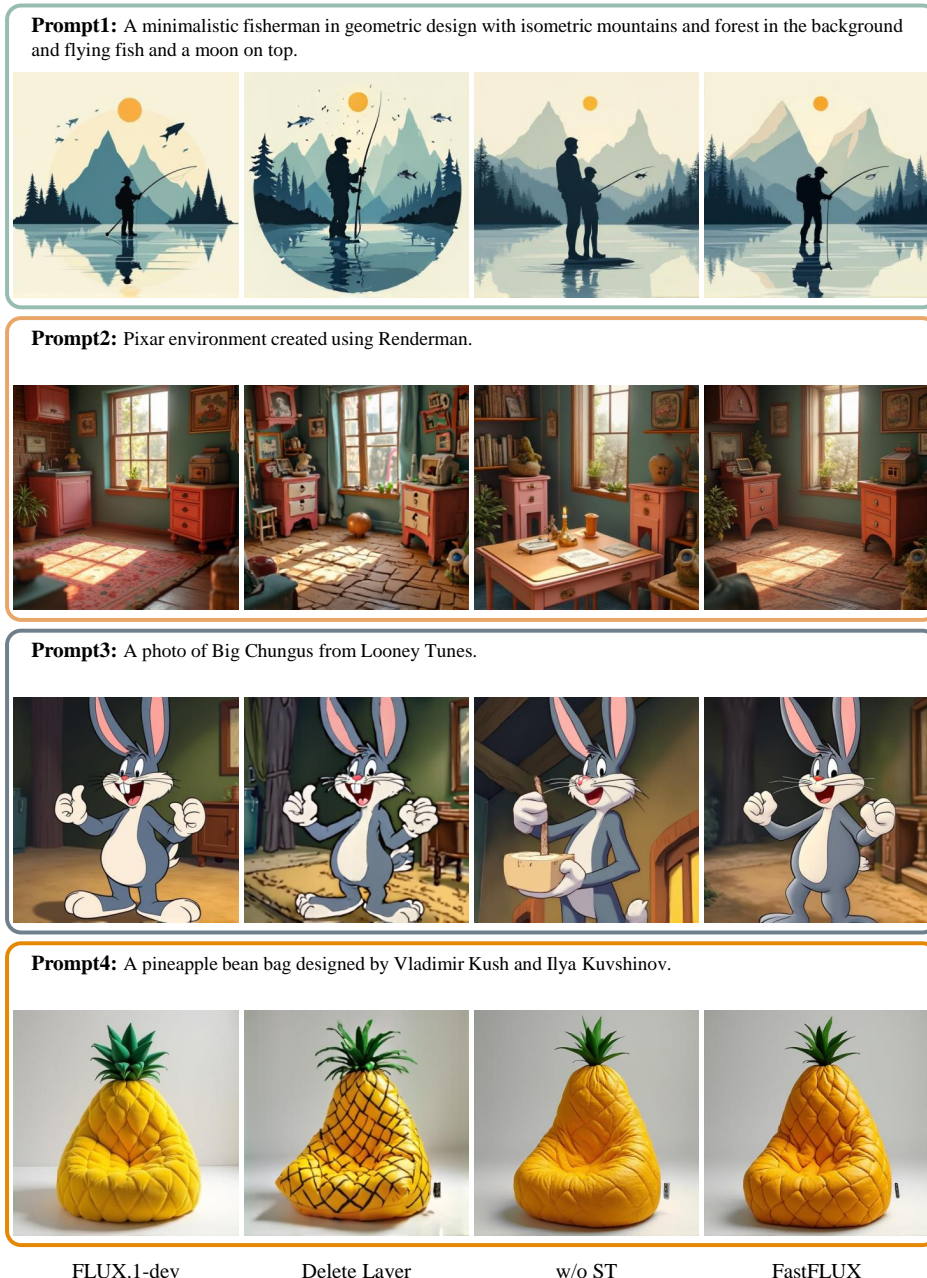


Figure 9: Visual comparison of image generations across four prompts (rows) and four methods (columns). From left to right: baseline output, result after direct layer deletion, result using naive linear replacement without our sandwich training strategy, and our proposed method. Our method best preserves the original visual characteristics of the baseline, demonstrating the effectiveness of both **ST** and **BRL** in maintaining image fidelity.

means that most blocks have a relatively small impact on the final generation, indicating room for optimization. Figure 10 shows a comparison of image generation results after removing layers of different importance. It can be observed that when important layers are removed, the model fails to generate images properly, while the generation results are almost unaffected when less important layers are removed. This validates the rationale behind our determination of layer importance.

Visual Analysis of Multiple Replacement Strategies. To better understand the visual impact of different block replacement strategies, we present a qualitative comparison across four prompts and

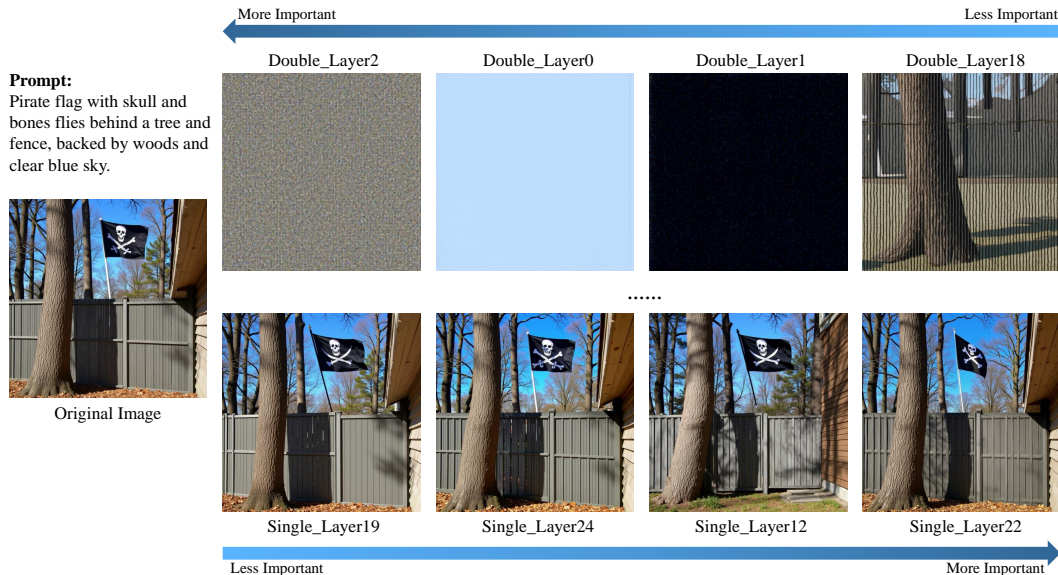


Figure 10: Visual impact of removing layers with different importance scores. The leftmost image shows the original output generated by the FLUX.1-dev model. The top row on the right shows the results after individually removing the four most important layers, while the bottom row shows the results after removing the four least important layers. Removing highly important layers significantly degrades generation quality, whereas removing low-importance layers has minimal visual impact. The visual contrast provides strong evidence that layers contribute unequally to model performance, validating the effectiveness of importance-aware layer pruning.

four methods in Figure 9. Each row corresponds to a prompt, and each column represents a different approach: the baseline model without any modification, direct deletion of selected blocks, block-wise linear replacement without ST, and our proposed method combining BRLL and ST. Visual results show that our method best preserves the original image characteristics. Direct deletion of blocks frequently results in noticeable texture degradation or missing structural elements, suggesting that individual blocks have varying levels of importance in preserving generation quality. Replacing blocks with linear layers without applying ST results in images that exhibit redundant patterns or positional artifacts, highlighting the limitations of naive replacement. In comparison, our full approach, which incorporates both BRLL and ST, produces images that are visually closest to the baseline. This demonstrates that BRLL provides a viable lightweight substitute for full blocks, and that ST is essential for stabilizing the training and aligning the replacement layers with the original model distribution. Together, these components effectively enhance inference efficiency while minimizing quality degradation.

5 Conclusion

In this work, we propose FastFLUX, a novel architecture-level pruning framework for efficient compression of large-scale diffusion models. By applying Block-wise Replacement with Linear Layers and introducing Sandwich Training for localized supervision, FastFLUX reduces inference cost and training overhead while maintaining high image quality. Even with 20% of the hierarchy pruned, it remains robust in generation and structural consistency. Extensive experiments demonstrated FastFLUX’s effectiveness and generalizability across different models, offering a streamlined and flexible paradigm for efficient compression and acceleration of T2I diffusion models.

References

- [1] Dongzhi Jiang, Ziyu Guo, Renrui Zhang, Zhuofan Zong, Hao Li, Le Zhuo, Shilin Yan, Pheng-Ann Heng, and Hongsheng Li. T2i-r1: Reinforcing image generation with collaborative semantic-level and token-level cot, 2025.
- [2] Patrick Esser, Sumith Kulal, Andreas Blattmann, Rahim Entezari, Jonas Müller, Harry Saini, Yam Levi, Dominik Lorenz, Axel Sauer, Frederic Boesel, et al. Scaling rectified flow transformers for high-resolution image synthesis. In *Forty-first international conference on machine learning*, 2024.
- [3] Dustin Podell, Zion English, Kyle Lacey, Andreas Blattmann, Tim Dockhorn, Jonas Müller, Joe Penna, and Robin Rombach. SDXL: Improving latent diffusion models for high-resolution image synthesis. In *The Twelfth International Conference on Learning Representations*, 2024.
- [4] Axel Sauer, Dominik Lorenz, Andreas Blattmann, and Robin Rombach. Adversarial diffusion distillation, 2023.
- [5] Junsong Chen, Jincheng Yu, Chongjian Ge, Lewei Yao, Enze Xie, Yue Wu, Zhongdao Wang, James Kwok, Ping Luo, Huchuan Lu, and Zhenguo Li. Pixart- α : Fast training of diffusion transformer for photorealistic text-to-image synthesis, 2023.
- [6] Lvmin Zhang, Anyi Rao, and Maneesh Agrawala. Adding conditional control to text-to-image diffusion models, 2023.
- [7] Yanbing Zhang, Mengping Yang, Qin Zhou, and Zhe Wang. Attention calibration for disentangled text-to-image personalization, 2024.
- [8] Agneet Chatterjee, Gabriela Ben Melech Stan, Estelle Aflalo, Sayak Paul, Dhruva Ghosh, Tejas Gokhale, Ludwig Schmidt, Hannaneh Hajishirzi, Vasudev Lal, Chitta Baral, and Yezhou Yang. Getting it right: Improving spatial consistency in text-to-image models, 2024.
- [9] William Peebles and Jun-Yan Xie. Scalable diffusion models with transformers. *arXiv preprint arXiv:2212.09748*, 2022.
- [10] Black Forest Labs. Flux. <https://github.com/black-forest-labs/flux>, 2024.
- [11] Muyang Li, Yujun Lin, Zhekai Zhang, Tianle Cai, Junxian Guo, Xiuyu Li, Enze Xie, Chenlin Meng, Jun-Yan Zhu, and Song Han. SVDQuant: Absorbing outliers by low-rank component for 4-bit diffusion models. In *The Thirteenth International Conference on Learning Representations*, 2025.
- [12] Victor Sanh, Lysandre Debut, Julien Chaumond, and Thomas Wolf. Distilbert, a distilled version of bert: smaller, faster, cheaper and lighter, 2020.
- [13] Chenlin Meng, Robin Rombach, Ruiqi Gao, Diederik P. Kingma, Stefano Ermon, Jonathan Ho, and Tim Salimans. On distillation of guided diffusion models, 2023.
- [14] Wujie Sun, Defang Chen, Can Wang, Deshi Ye, Yan Feng, and Chun Chen. Accelerating diffusion sampling with classifier-based feature distillation, 2023.
- [15] Jonas Kohler, Albert Pumarola, Edgar Schönfeld, Artsiom Sanakoyeu, Roshan Sumbaly, Peter Vajda, and Ali Thabet. Imagine flash: Accelerating emu diffusion models with backward distillation, 2024.
- [16] Tri Dao, Daniel Y. Fu, Stefano Ermon, Atri Rudra, and Christopher Ré. Flashattention: Fast and memory-efficient exact attention with io-awareness, 2022.
- [17] Tri Dao. Flashattention-2: Faster attention with better parallelism and work partitioning, 2023.
- [18] Iz Beltagy, Matthew E. Peters, and Arman Cohan. Longformer: The long-document transformer, 2020.
- [19] Manzil Zaheer, Guru Guruganesh, Avinava Dubey, Joshua Ainslie, Chris Alberti, Santiago Ontanon, Philip Pham, Anirudh Ravula, Qifan Wang, Li Yang, and Amr Ahmed. Big bird: Transformers for longer sequences, 2021.
- [20] Tim Salimans and Jonathan Ho. Progressive distillation for fast sampling of diffusion models, 2022.
- [21] Jianze Li, Jiezhong Cao, Yong Guo, Wenbo Li, and Yulun Zhang. One diffusion step to real-world super-resolution via flow trajectory distillation, 2025.
- [22] Wenhao Hu, Perry Gibson, and José Cano. ICE-pick: Iterative cost-efficient pruning for DNNs. In *ICML 2023 Workshop Neural Compression: From Information Theory to Applications*, 2023.

- [23] Svetlana Pavlitska, Oliver Bagge, Federico Peccia, Toghrul Mammadov, and J. Marius Zöllner. Iterative filter pruning for concatenation-based cnn architectures, 2024.
- [24] John Tan Chong Min and Mehul Motani. Dropnet: reducing neural network complexity via iterative pruning. In *Proceedings of the 37th International Conference on Machine Learning, ICML'20*. JMLR.org, 2020.
- [25] Stijn Verdenius, Maarten Stol, and Patrick Forré. Pruning via iterative ranking of sensitivity statistics, 2020.
- [26] Mingjie Sun, Zhuang Liu, Anna Bair, and J. Zico Kolter. A simple and effective pruning approach for large language models, 2024.
- [27] Nyalalani Smarts, Rajalakshmi Selvaraj, and Venumadhav Kuthadi. A conceptual framework for efficient and sustainable pruning techniques in deep learning models. *Journal of Computer Science*, 21(5):1113–1128, Apr 2025.
- [28] Jun Liu, Zhenglun Kong, Pu Zhao, Changdi Yang, Hao Tang, Xuan Shen, Geng Yuan, Wei Niu, Wenbin Zhang, Xue Lin, Dong Huang, and Yanzhi Wang. Toward adaptive large language models structured pruning via hybrid-grained weight importance assessment, 2025.
- [29] Yizhuo Ding, Xinwei Sun, Yanwei Fu, and Guosheng Hu. Revisiting large language model pruning using neuron semantic attribution, 2025.
- [30] Elias Frantar and Dan Alistarh. Sparsegpt: Massive language models can be accurately pruned in one-shot, 2023.
- [31] Edward J. Hu, Yelong Shen, Phillip Wallis, Zeyuan Allen-Zhu, Yuanzhi Li, Shean Wang, Lu Wang, and Weizhu Chen. Lora: Low-rank adaptation of large language models, 2021.
- [32] Jonathan Ho, Ajay Jain, and Pieter Abbeel. Denoising diffusion probabilistic models. *Advances in Neural Information Processing Systems*, 33:6840–6851, 2020.
- [33] Robin Rombach, Andreas Blattmann, Dominik Lorenz, Patrick Esser, and Björn Ommer. High-resolution image synthesis with latent diffusion models. *Proceedings of the IEEE/CVF Conference on Computer Vision and Pattern Recognition*, pages 10684–10695, 2022.
- [34] Geoffrey Hinton, Oriol Vinyals, and Jeff Dean. Distilling the knowledge in a neural network. *arXiv preprint arXiv:1503.02531*, 2015.
- [35] Benoit Jacob, Skirmantas Kligys, Bo Chen, Menglong Zhu, Matthew Tang, Andrew Howard, Hartwig Adam, and Dmitry Kalenichenko. Quantization and training of neural networks for efficient integer-arithmetic-only inference. *Proceedings of the IEEE/CVF Conference on Computer Vision and Pattern Recognition*, pages 2704–2713, 2018.
- [36] Barret Zoph, Vijay Vasudevan, Jonathon Shlens, and Quoc V Le. Learning transferable architectures for scalable image recognition. In *Proceedings of the IEEE conference on computer vision and pattern recognition*, pages 8697–8710, 2018.
- [37] Hao Li, Asim Kadav, Igor Durdanovic, Hanan Samet, and Hans Peter Graf. Pruning filters for efficient convnets. In *International Conference on Learning Representations*, 2017.
- [38] Yihui He, Xiangyu Zhang, and Jian Sun. Channel pruning for accelerating very deep neural networks. In *Proceedings of the IEEE international conference on computer vision*, pages 1389–1397, 2017.
- [39] Krzysztof Choromanski, Valerii Likhoshesterov, David Dohan, Xingyou Song, Aditya Gane, Tamas Sarlos, Peter Hawkins, Jared Davis, Afroz Mohiuddin, Lukasz Kaiser, David Belanger, Lucy Colwell, and Adrian Weller. Rethinking attention with performers. In *International Conference on Learning Representations*, 2021.
- [40] Yi Tay, Mostafa Dehghani, Samira Abnar, Yikang Shen, Dara Bahri, Philip Pham, Jinfeng Rao, Liu Yang, Sebastian Ruder, and Donald Metzler. Long range arena: A benchmark for efficient transformers. *arXiv preprint arXiv:2011.04006*, 2020.
- [41] Surat Teerapittayanon, Bradley McDanel, and H. T. Kung. Branchynet: Fast inference via early exiting from deep neural networks. In *2016 23rd International Conference on Pattern Recognition (ICPR)*, pages 2464–2469. IEEE, 2016.

- [42] Maha Elbayad, Jiatao Gu, Edouard Grave, and Michael Auli. Depth-adaptive transformer. In *Proceedings of the 2019 Conference on Empirical Methods in Natural Language Processing (EMNLP)*, pages 2755–2764, 2019.
- [43] Angela Fan, Edouard Grave, and Armand Joulin. Reducing transformer depth on demand with structured dropout. In *International Conference on Learning Representations*, 2020.
- [44] Taeyong Kim et al. Learned depth: Dynamic depth for better generalization in continued fraction expansion. *arXiv preprint arXiv:2109.04661*, 2021.
- [45] Yongming Rao, Wenliang Zhao, Zheng Zhu, Jiwen Lu, Jie Zhou, and Houqiang Li. Dynamicvit: Efficient vision transformers with dynamic token sparsification. In *Advances in Neural Information Processing Systems*, volume 34, pages 13937–13949, 2021.
- [46] Jinhwi Park, Jaehoon Choi, and Seungryong Kim. Depth prompting for sensor-agnostic depth estimation. *arXiv preprint arXiv:2210.02291*, 2022.
- [47] Martin Heusel, Hubert Ramsauer, Thomas Unterthiner, Bernhard Nessler, and Sepp Hochreiter. Gans trained by a two time-scale update rule converge to a local nash equilibrium, 2018.
- [48] Alec Radford, Jong Wook Kim, Chris Hallacy, Aditya Ramesh, Gabriel Goh, Sandhini Agarwal, Girish Sastry, Amanda Askell, Pamela Mishkin, Jack Clark, Gretchen Krueger, and Ilya Sutskever. Learning transferable visual models from natural language supervision, 2021.
- [49] Aditya Ramesh, Mikhail Pavlov, Gabriel Goh, Scott Gray, Chelsea Voss, Alec Radford, Mark Chen, and Ilya Sutskever. Zero-shot text-to-image generation, 2021.
- [50] Robin Rombach, Andreas Blattmann, Dominik Lorenz, Patrick Esser, and Björn Ommer. High-resolution image synthesis with latent diffusion models, 2022.
- [51] Xiaoshi Wu, Yiming Hao, Keqiang Sun, Yixiong Chen, Feng Zhu, Rui Zhao, and Hongsheng Li. Human preference score v2: A solid benchmark for evaluating human preferences of text-to-image synthesis, 2023.
- [52] Dhruva Ghosh, Hanna Hajishirzi, and Ludwig Schmidt. Geneval: An object-focused framework for evaluating text-to-image alignment, 2023.
- [53] Zhuang Liu, Mingjie Sun, Tinghui Zhou, Gao Huang, and Trevor Darrell. Rethinking the value of network pruning, 2019.